



Published in final edited form as:

*Cell Cycle*. 2006 September ; 5(17): 1940–1945.

## Constitutive Histone H2AX Phosphorylation and ATM Activation, the Reporters of DNA Damage by Endogenous Oxidants

Toshiki Tanaka<sup>1,2</sup>, H. Dorota Halicka<sup>1</sup>, Xuan Huang<sup>1</sup>, Frank Traganos<sup>1</sup>, and Zbigniew Darzynkiewicz<sup>1,\*</sup>

<sup>1</sup>Brander Cancer Research Institute and Department of Pathology; New York Medical College; Valhalla, New York USA

<sup>2</sup>First Department of Surgery; Yamaguchi University School of Medicine; Ube, Yamaguchi Japan

### Abstract

DNA in live cells undergoes continuous oxidative damage caused by metabolically generated endogenous as well as external oxidants and oxidant-inducers. The cumulative oxidative DNA damage is considered the key factor in aging and senescence while the effectiveness of anti-aging agents is often assessed by their ability to reduce such damage. Oxidative DNA damage also preconditions cells to neoplastic transformation. Sensitive reporters of DNA damage, particularly the induction of DNA double-strand breaks (DSBs), are activation of ATM, through its phosphorylation on *Ser* 1981, and phosphorylation of histone H2AX on *Ser* 139; the phosphorylated form of H2AX has been named  $\gamma$ H2AX. We review the observations that constitutive ATM activation (CAA) and H2AX phosphorylation (CHP) take place in normal cells as well in the cells of tumor lines untreated by exogenous genotoxic agents. We postulate that CAA and CHP, which have been measured by multiparameter cytometry in relation to the cell cycle phase, are triggered by oxidative DNA damage. This review also presents the findings on differences in CAA and CHP in various cell lines as well as on the effects of several agents and growth conditions that modulate the extent of these histone and ATM modifications. Specifically, described are effects of the reactive oxygen species (ROS) scavenger N-acetyl-L-cysteine (NAC), and the glutathione synthetase inhibitor buthionine sulfoximine (BSO) as well as suppression of cell metabolism by growth at higher cell density or in the presence of the glucose antimetabolite 2-deoxy-D-glucose. Collectively, the reviewed data indicate that multiparameter cytometric measurement of the level of CHP and/or CAA allows one to estimate the extent of ongoing oxidative DNA damage and to measure the DNA protective-effects of antioxidants or agents that reduce or amplify generation of endogenous ROS.

### Keywords

aging; senescence; DNA replication; DNA double-strand breaks; cell cycle; free radicals; reactive oxygen species (ROS); reactive oxygen intermediates (ROIs); anti-oxidants; oxidative stress

## DNA DAMAGE BY ENDOGENOUS OXIDANTS

Being continuously exposed to oxidants produced during metabolic activity and to external oxidants or oxidant-inducers, DNA within cells undergoes oxidative damage. Estimates of the extent of endogenous DNA damage vary widely.<sup>1–5</sup> According to one of the relatively

low estimates, during a single cell cycle of average duration (24 h) approximately 5,000 DNA single-strand lesions (SSLs) are generated per nucleus by endogenous reactive oxygen species (ROS).<sup>5</sup> The SSLs consist of single-strand breaks, apurinic/aprimidinic sites, oxidation products such as 8-oxoguanine and thymine glycol, and some alkylation products.<sup>1–5</sup> Approximately 1% of these SSLs become converted to DNA double-strand breaks (DSBs), predominantly at the time of DNA replication, while the remaining 99% are repaired by essentially error-free mechanisms. Thus, on average, about 50 DSBs (“endogenous DSBs”) per nucleus (~0.8 DSBs per 10<sup>8</sup> bp) are generated during a single cell cycle in human cells.<sup>5</sup> Recombinatorial repair (also known as template-assisted repair or homologous recombination repair) and nonhomologous DNA-end joining (NHEJ) are two major pathways for repair of DSBs. The NHEJ pathway is error-prone, often resulting in deletion of a few base pairs.<sup>6,7</sup> This leads to accumulation of DNA damage with each sequential cell cycle, which is considered to be the primary cause of cell aging and senescence.<sup>4,8,9</sup> The cumulative DNA damage also promotes development of preneoplastic changes. Many strategies aimed at slowing down the aging process or preventing cancer are based on protection of DNA from oxidative damage, primarily by scavenging the endogenous oxidants. While approaches to measure the presence of oxidants within the cell have been developed,<sup>10,11</sup> the possibilities for detecting DSBs generated by endogenous oxidants are limited. DNA damage assessment by the comet methodology<sup>12</sup> is rather cumbersome, lacks the desired sensitivity and cannot provide information on the relationship between DNA damage and the cell cycle phase in which the damage occurred. The detection of DSBs by the TUNEL assay, while highly useful in identifying DNA fragmentation that occurs during apoptosis,<sup>13</sup> also is not sensitive enough to detect DNA damage induced by endogenous oxidants. Low sensitivity is also the Achilles heel of other methods developed to measure in situ DNA damage and repair.<sup>14</sup> Methods that measure DNA damage in bulk rather than in situ do not provide information on the response of individual cells, cell population heterogeneity or the relationship of DNA damage to cell cycle phase.

## HISTONE H2AX PHOSPHORYLATION AND ATM ACTIVATION, THE MARKERS OF DNA DAMAGE

One of the variants of the nucleosome core histone H2A, histone H2AX undergoes phosphorylation on *Ser* 139 in response to DNA damage, particularly if the damage involves formation of DNA double-strand breaks (DSBs).<sup>15,16</sup> Its phosphorylation, in nucleosomes located within a megabase domain of DNA on each side of the DSB,<sup>17</sup> is mediated by the PI-3-like kinases ATM-<sup>18</sup> ATR-<sup>19</sup> and/or DNA-dependent protein kinase (DNA-PK).<sup>20</sup> The *Ser*-139-phosphorylated H2AX has been named  $\gamma$ H2AX.<sup>14</sup> The presence of  $\gamma$ H2AX manifests in the form of distinct nuclear  $\gamma$ H2AX immunofluorescent (IF) foci.<sup>15–17</sup> Several signaling and repair proteins including the M/R/N complex (Mre11/Rad50/Nbs1), Brca1 and the p53 binding protein 1 (53BP1) colocalize with phosphorylated H2AX at the foci.<sup>21–24</sup> Phosphorylation of H2AX is considered to be a specific reporter of DSBs.<sup>15–17,25–27</sup> Cytometric detection of phosphorylated H2AX combined with analysis of cellular DNA content provides an assay of DNA damage (e.g., induced by genotoxic agents such as some antitumor drugs) in relation to the cell cycle phase. An example of induction of H2AX phosphorylation in cells treated with DNA topoisomerase I inhibitor topotecan (Tpt) is presented in Figure 1.

H2AX is also phosphorylated in physiological recombinatorial events such as in V(D)J and class-switch recombination during immune system development and also at sites of DSB formation in meiosis.<sup>28–31</sup> Likewise, DSBs generated during DNA fragmentation in apoptotic cells induce phosphorylation of H2AX, the extent of which, however, is much greater compared to its phosphorylation induced by exogenous genotoxic agents.<sup>32–34</sup> In

fact, the large difference in the degree of H2AX phosphorylation makes it possible, based on the intensity of  $\gamma$ H2AX IF, to discriminate between the apoptotic cells and the cells with primary DSBs generated by DNA damaging agents such as ionizing radiation or by DNA topoisomerase inhibitors.<sup>33–35</sup>

DNA damage triggers activation of *Ataxia telangiectasia* mutated (ATM) through its phosphorylation on Ser1981, and, as noted, H2AX is a substrate of this kinase.<sup>18,36–40</sup> Whereas H2AX can be phosphorylated by ATR in response to other types of DNA damage, its phosphorylation when mediated by ATM appears to be strongly linked to the induction of DSBs.<sup>36–40</sup> Thus, ATM activation and H2AX phosphorylation observed within the same cells provide strong evidence of the induction of DSBs.<sup>37–41</sup> The immunocytochemical detection of  $\gamma$ H2AX concurrent with activated ATM using Abs tagged with a fluorochrome of the same emission wavelength is a very sensitive assay to detect DNA damage that involves formation of DSBs.<sup>41</sup> Figure 1 illustrates the induction of ATM activation concurrent with H2AX phosphorylation, selectively in S-phase cells, by Tpt.<sup>41</sup>

## CONSTITUTIVE HISTONE H2AX PHOSPHORYLATION (CHP) AND ACTIVATION OF ATM (CAA)

Given the above, it could be expected that during unperturbed growth of cells (i.e., in the absence of any exogenous genotoxic agents) there will be a background level of H2AX phosphorylation, and perhaps also activation of ATM, reflecting the cell response to oxidative DNA damage induced by endogenous oxidants that arise from the metabolic activity occurring during cell cycle progression. Indeed, we<sup>33,43</sup> and others<sup>42</sup> observed that in untreated, normal cells as well in the cells of various tumor lines, a fraction of the histone H2AX molecules remain phosphorylated. The extent of this constitutive H2AX phosphorylation (CHP) varies depending on the cell type (line) and on cell cycle phase.<sup>33,43</sup> Figure 2 illustrates CHP variability among 6 different cell lines and in normal human bronchial epithelial cells (NHBE), the latter having the highest level of  $\gamma$ H2AX expression. Cells also constitutively express activated ATM and, as with CHP, the degree of constitutive ATM activation (CAA) differs depending on cell type and cell cycle phase.<sup>40,43</sup>

It should be stressed, however, that mechanisms of CHP and CAA are different in interphase and in mitotic cells.<sup>44–48</sup> While CHP and CAA in interphase cells most likely reflect a response to DNA damage that may involve the presence of DSBs, in mitotic cells these events may be associated with chromatin condensation. For example, the induction of premature chromosomes condensation triggers CHP and CAA even though there is no evidence of DSB formation.<sup>48</sup> It has been speculated that the changes in chromatin structure during mitosis associated with the induction of torsional stress on the DNA double helix that make it more sensitive to single-strand nucleases<sup>49</sup> or susceptible to denaturation,<sup>50,51</sup> may be the signal triggering H2AX phosphorylation and ATM activation.<sup>48</sup> Furthermore, in mitotic cells, activated ATM is also localized at centrosomes where its function may be associated with the monitoring of mitotic spindle integrity.<sup>46</sup> Phosphorylation of H2AX at mitosis is also a response to telomere shortening and is associated with induction of cell senescence or apoptosis.<sup>48</sup>

The present review is focused on CHP and CAA in interphase cells and summarizes the findings that provide the linkage suggesting that these events reflect DNA damage by endogenous oxidants. The reviewed data also underscore the fact that multiparameter cytometric analysis of CHP and CAA provides a sensitive and convenient assay for the DNA protective properties of antioxidants and potential anti-aging agents.

## THE RELATIONSHIP BETWEEN H2AX PHOSPHORYLATION AND TP53

As mentioned, the presence of the phosphorylated form of H2AX ( $\gamma$ H2AX) has been detected immunocytochemically in a variety of cell types not subjected to treatment with any genotoxic agent.<sup>33,42,52</sup> The bivariate distributions of cellular DNA content vs  $\gamma$ H2AX immunofluorescence (IF) revealed CHP in relation to cell cycle phase (Fig. 2). It is quite evident from these distributions that the level of CHP varies markedly depending on the cell type. For example NHBE cells or cells from the A549 or DU145 lines have distinctly higher expression of  $\gamma$ H2AX than the cells from Jurkat, MCF-7 or HL-60 lines. Interestingly, among a variety of cell types analyzed, the cells harboring wt TP53 had generally more elevated levels of CHP compared with the cells that had either mutated TP53 or were null for TP53.<sup>52</sup> Thus, among the human lymphoblastoid cell lines derived from WIL2 cells, the TK6 cells having wt TP53 showed significantly higher expression of  $\gamma$ H2AX than NH32 cells, the TP53 knock-out derived from TK6, or WTK1, a WIL2-derived line harboring a homozygous mutant of TP53.<sup>52</sup> The degree of CHP was also low in TP53 null HL-60 cells.<sup>52</sup> The level of reactive oxygen species detected by the cell's ability to oxidize carboxyl-dichlorodihydrofluorescein diacetate,<sup>10,11</sup> however, was not significantly different in any of these cell lines, which would suggest that oxidative DNA damage was similar in these lines. The observed higher level of CHP in cells harboring wt TP53, therefore, may indicate that TP53 plays a role in facilitating histone H2AX phosphorylation, the step that mobilizes the DNA repair machinery to the site of DSBs. This function of TP53 is compatible with its role in sensing oxidative DNA damage and facilitating base excision repair,<sup>53-55</sup> and also with its direct and rapid binding to sites of DSBs and interaction with  $\gamma$ H2AX.<sup>56</sup>

## SENSITIVITY OF CHP AND CAA TO N-ACETYL-L-CYSTEINE (NAC), AN ROS SCAVENGER

The level of CHP was markedly attenuated in the TK6 cells growing in the presence of NAC (Fig. 3). The effect was NAC concentration-dependent and was already apparent in cell treated with 10 mM concentration of this antioxidant. At 50 mM NAC, the mean  $\gamma$ H2AX IF of G<sub>2</sub>M cells was reduced by 48%, whereas the reduction of  $\gamma$ H2AX IF of G<sub>1</sub>- and S-phase cells was 37 and 36%, respectively. Significant reduction of CHP was also observed in A549 and NHBE cells that were grown in the presence of NAC.<sup>43</sup> In contrast, growth of A549 cells in the presence of buthionine sulfoximine (BSO), an inhibitor of glutathione synthetase, for the approximate duration of one cell cycle, led to a distinct rise in the level of CHP.<sup>43</sup> The BSO-induced CHP increase was more pronounced for cells in S and G<sub>2</sub>M phase (61–62%) than for G<sub>1</sub> phase cells (30%). All these data, collectively, strongly suggest that the CHP observed in untreated, proliferating cells is a reflection of the ongoing DNA damage caused by endogenous oxidants. Their scavenging by NAC, or elevation as a result of depletion of glutathione by BSO, modulates the extent of CHP accordingly.

The level of CAA was also markedly diminished in the TK6 cells treated with NAC (Fig. 4). As in the case of CHP, the reduction of CAA was NAC concentration-dependent. At 50 mM NAC, the mean ATM-S1981<sup>P</sup> IF of G<sub>1</sub>-, S- and G<sub>2</sub>- phase cell populations was diminished by 51–53% compared to the untreated cells. It should be noted however, that the ATM-S1981<sup>P</sup> IF of mitotic cells essentially was unaffected by NAC.

## CHP AND CAA IN CELLS WITH DIFFERENT METABOLIC ACTIVITY

Given that CHP and CAA reflect DNA damage caused by endogenous oxidants generated during metabolic activity it would be expected that the level CHP and CAA may be correlated with the overall rate of cell metabolism. Therefore, it seemed important to

determine whether suppression of metabolic activity would lead to a decrease in the levels of CHP and CAA. Towards this end, the levels of CHP and CAA have been assessed in cells that were grown for up to 24 h in the presence of the glucose antimetabolite 2-deoxy-D-glucose (2-DG).<sup>57</sup> 2-DG competitively inhibits the uptake and utilization of glucose thereby suppressing glycolysis and reducing energy production in mitochondria that should lead to a decrease in production of ROS.<sup>58–60</sup> It has been suggested that, similar to caloric restriction or reduced oxygen levels,<sup>61</sup> a nontoxic anti-metabolite might be used as a “caloric restriction mimetic” to lower the extent of DNA damage by oxidative stress and, as a result, expand the life span of cells or organisms.<sup>58,62</sup> The studies<sup>57</sup> were carried out on three different human lymphoblastoid cell lines (TK6, NH32 and WTK1), which as mentioned above, differed in their TP53 status.<sup>53</sup> A distinct attenuation of CHP and CAA in cells growing in the presence of 2-DG was observed for all three lines; a significant decrease was observed as early as 4 h following exposure to 2-DG.<sup>58</sup> This data provided further support for the notion that CHP is a reporter of oxidative DNA damage caused by ROS during the metabolic processes fueled by glycolysis when cells progress through the cell cycle. Additionally, the data suggested that ATM either alone or in concert with other PI-3-like kinase(s), mediated CHP.<sup>57</sup> Figure 5 shows the data selected from this report<sup>57</sup> and illustrates the effect of exposure of WTK1 cells to 2-DG for 24 h on the level of CHP and CAA. It is quite evident that the cells growing in the presence of 2-DG had both markedly diminished CHP and CAA. The reduction of CAA was more pronounced (45–51%) than the decrease of CHP (27–43%). These observations are consistent with our recent findings that growth in the presence of 2-DG reduced the level of ROS as reflected by a decrease in cell ability to oxidize carboxyl-dichlorodihydrofluorescein diacetate (unpublished).

Cell growth at higher cell density in cultures reduces their proliferation and also attenuates their metabolic activity as reflected by retention of rhodamine 123 a probe of mitochondrial mass and potential, as well as by reduced rates of RNA and protein synthesis.<sup>63–65</sup> Figure 6 presents the level CHP and CAA in TK6 cells growing at densities  $2 \times 10^5$ ,  $10^6$  and  $2 \times 10^6$  cells/ml, respectively. These data demonstrate that CHP and CAA levels were distinctly reduced in cells maintained at higher densities. As in the case of cell growth in the presence of 2-DG, the reduction was more pronounced for CAA (40–46%) than for CHP (17–27%). It should be stressed that the observed reduction of CHP and CAA induced by 2-DG<sup>57</sup> or by growth at higher densities was not accompanied by any cytotoxic effects. In the case of growth at higher densities a moderate decrease in the proportion of S and G<sub>2</sub>M phase cells was apparent (Fig. 6, see the insets), consistent with the reduced rate of proliferation at higher cell densities.<sup>65</sup>

## Acknowledgments

This work was supported by NCI RO1 CA 28704.

## References

1. Barzilai A, Yamamoto K. DNA damage responses to oxidative stress. *DNA repair (Amst)*. 2004; 3:1109–15. [PubMed: 15279799]
2. Nohl H. Generation of superoxide radicals as byproducts of cellular respiration. *Ann Biol Clin*. 1994; 52:199–204.
3. Moller P, Loft S. Interventions with antioxidants and nutrients in relation to oxidative DNA damage and repair. *Mutat Res*. 2004; 551:79–89. [PubMed: 15225583]
4. Beckman KB, Ames BN. Oxidative decay of DNA. *J Biol Chem*. 1997; 272:13300–5.
5. Vilenchik MM, Knudson AG. Endogenous DNA double-strand breaks: Production, fidelity of repair, and induction of cancer. *Proc Natl Acad Sci USA*. 2003; 100:12871–6. [PubMed: 14566050]

6. Pastwa E, Blasiak J. Nonhomologous DNA end joining. *Acta Biochim Pol.* 2003; 50:891–908. [PubMed: 14739985]
7. Jeggo PA, Lobrich M. Artemis links ATM to double strand end rejoining. *Cell Cycle.* 2005; 4:359–62. [PubMed: 15684609]
8. Gorbunova V, Seluanov A. Making ends meet in old age: DSB repair and aging. *Mech Ageing Dev.* 2005; 126:621–8. [PubMed: 15888314]
9. Karanjawala ZE, Lieber MR. DNA damage and aging. *Mech Ageing Dev.* 2004; 125:405–16. [PubMed: 15272504]
10. Weir IE, Pham NA, Hedley DW. Oxidative stress is generated via the mitochondrial respiratory chain during plant cell apoptosis. *Cytometry.* 2003; 54A:109–17. [PubMed: 12879457]
11. Pham NA, Robinson BH, Hedley DW. Simultaneous detection of mitochondrial respiratory chain activity and reactive oxygen in digitonin-permeabilized cells using flow cytometry. *Cytometry.* 2000; 41:245–51. [PubMed: 11084609]
12. Olive PL, Durand RE, Banath JP, Johnston PJ. Analysis of DNA damage in individual cells. *Methods Cell Biol.* 2001; 64:235–49. [PubMed: 11070842]
13. Gorczyca W, Bruno S, Darzynkiewicz RJ, Gong J, Darzynkiewicz Z. DNA strand breaks occurring during apoptosis: Their early in situ detection by the terminal deoxynucleotidyl transferase and nick translation assays and prevention by serine protease inhibitors. *Int J Onc.* 1992; 1:639–48.
14. Didenko, VD. *Methods and Protocols.* Totowa, NJ: Humana Press; 2002. In situ detection of DNA damage.
15. Rogakou EP, Pilch DR, Orr AH, Ivanova VS, Bonner WM. DNA double-stranded breaks induce histone H2AX phosphorylation on serine 139. *J Biol Chem.* 1998; 273:5858–68. [PubMed: 9488723]
16. Sedelnikova OA, Rogakou EP, Panuytin IG, Bonner W. Quantitative detection of <sup>125</sup>IUdr-induced DNA double-strand breaks with  $\gamma$ -H2AX antibody. *Radiation Res.* 2002; 158:486–92. [PubMed: 12236816]
17. Rogakou EP, Boon C, Redon C, Bonner WM. Megabase chromatin domains involved in DNA double-strand breaks in vivo. *J Cell Biol.* 1999; 146:905–16. [PubMed: 10477747]
18. Burma S, Chen BP, Murphy M, Kurimasa A, Chen DJ. ATM phosphorylates histone H2AX in response to DNA double-strand breaks. *J Biol Chem.* 2001; 276:42462–7. [PubMed: 11571274]
19. Anderson L, Henderson C, Adachi Y. Phosphorylation and rapid relocalization of 53BP1 to nuclear foci upon DNA damage. *Mol Cell Biol.* 2001; 21:1719–9. [PubMed: 11238909]
20. Park EJ, Chan DW, Park JH, Oettinger MA, Kwon J. DNA-PK is activated by nucleosomes and phosphorylated H2AX within the nucleosomes in an acetylation-dependent manner. *Nucleic Acids Res.* 2003; 31:6819–27. [PubMed: 14627815]
21. Paull TT, Rogakou EP, Yamazaki V, Kirchgesser CU, Gellert M, Bonner WM. A critical role for histone H2AX in recruitment of repair factors to nuclear foci after DNA damage. *Curr Biol.* 2000; 10:886–95. [PubMed: 10959836]
22. Foster ER, Downs JA. Histone H2AX phosphorylation in DNA double-strand break repair. *FEBS J.* 2005; 272:3231–40. [PubMed: 15978030]
23. Downs JA, Cote J. Dynamics of chromatin during the repair of DNA double-strand breaks. *Cell Cycle.* 2005; 4:1373–6. [PubMed: 16205111]
24. Furuta T, Takemura H, Liao ZY, Aune GJ, Redon C, Sedelnikova OA, Pilch DR, Rogakou EP, Celeste A, Chen HT, Nussenzweig A, Aladjem MI, Bonner WM, Pommier Y. Phosphorylation of histone H2AX and activation of Mre11, Rad50, and Nbs1 in response to replication-dependent DNA double-strand breaks induced by mammalian topoisomerase I cleavage complexes. *J Biol Chem.* 2003; 278:20303–12. [PubMed: 12660252]
25. Takahashi A, Ohnishi T. Does  $\gamma$ H2AX foci formation depend on the presence of DNA double-strand breaks? *Cancer Letters.* 2005; 229:171–9. [PubMed: 16129552]
26. Banath JP, Olive PL. Expression of phosphorylated histone H2AX as a surrogate of cell killing by drugs that created DNA double-strand breaks. *Cancer Res.* 2003; 63:4347–50. [PubMed: 12907603]
27. Olive PL. Detection of DNA damage in individual cells by analysis of histone H2AX phosphorylation. *Methods Cell Biol.* 2004; 75:355–73. [PubMed: 15603433]

28. Jackson SP. DNA damage signaling and apoptosis. *Biochem Soc Transactions*. 2001; 29:655–61.
29. Fernandez-Capetillo O, Chen HT, Celeste A, Ward I, Romanienko P, Morales JC, Naka K, Xia Z, Camerini-Otero RD, Motoyama N, Carpenter PB, Bonner WM, Chen J, Nussenzweig A. DNA damage-induced G<sub>2</sub>-M checkpoint activation by histone H2AX and 53BP1. *Nature Cell Biol*. 2002; 4:993–7. [PubMed: 12447390]
30. Modesti M, Kanaar R. DNA repair: Spot(light)s on chromatin. *Curr Biol*. 2001; 11:R229–32. [PubMed: 11301269]
31. Sedelnikova OA, Pilch DR, Redon C, Bonner WM. Histone H2AX in DNA damage and repair. *Canc Biol Ther*. 2003; 2:233–5.
32. Huang X, Okafuji M, Traganos F, Luther E, Holden E, Darzynkiewicz Z. Assessment of histone H2AX phosphorylation induced by DNA topoisomerase I and II inhibitors topotecan and mitoxantrone and by DNA crosslinking agent cisplatin. *Cytometry*. 2004; 58A:99–110. [PubMed: 15057963]
33. Huang X, Halicka HD, Traganos F, Tanaka T, Kurose A, Darzynkiewicz Z. Cytometric assessment of DNA damage in relation to cell cycle phase and apoptosis. *Cell Proliferation*. 2005; 38:223–43. [PubMed: 16098182]
34. Huang X, Traganos F, Darzynkiewicz Z. DNA damage induced by DNA topoisomerase I-and topoisomerase II- inhibitors detected by histone H2AX phosphorylation in relation to the cell cycle phase and apoptosis. *Cell Cycle*. 2003; 2:614–19. [PubMed: 14504478]
35. Halicka HD, Huang X, Traganos F, King MA, Dai W, Darzynkiewicz Z. Histone H2AX phosphorylation after cell irradiation with UV-B: Relationship to cell cycle phase and induction of apoptosis. *Cell Cycle*. 2005; 4:339–45. [PubMed: 15655354]
36. Zhou BB, Elledge SJ. The DNA damage response: Putting checkpoints in perspective. *Nature*. 2000; 408:433–9. [PubMed: 11100718]
37. Ward IM, Minn K, Chen J. UV-induced ataxia-telangiectasia-mutated and Rad3-related (ATR) activation requires replication stress. *J Biol Chem*. 2004; 279:9677–80. [PubMed: 14742437]
38. Lee JH, Paull TT. ATM activation by DNA double-strand breaks through the Mre11-Rad50-Nbs1 complex. *Science*. 2005; 308:551–4. [PubMed: 15790808]
39. Abraham RT, Tibbetts RS. Guiding ATM to broken DNA. *Science*. 2005; 308:510–1. [PubMed: 15845843]
40. Bartkova J, Bakkenist CJ, Rajpert-De Meyts E, Skakkebaek NE, Sehested M, Lukas J, Kastan MB, Bartek J. ATM activation in normal human tissues and testicular cancer. *Cell Cycle*. 2005; 4:838–45. [PubMed: 15846060]
41. Tanaka T, Kurose A, Huang X, Dai W, Darzynkiewicz Z. ATM kinase activation and histone H2AX phosphorylation as indicators of DNA damage by DNA topoisomerase I inhibitor topotecan and during apoptosis. *Cell Proliferation*. 2006; 39:49–60. [PubMed: 16426422]
42. MacPhail SH, Banath JP, Yu Y, Chu E, Olive PL. Cell cycle-dependent expression of phosphorylated histone H2AX: Reduced expression in unirradiated but not X-irradiated G<sub>1</sub>-phase cells. *Radiat Res*. 2003; 159:759–67. [PubMed: 12751958]
43. Huang X, Tanaka T, Kurose A, Traganos F, Darzynkiewicz Z. Constitutive histone H2AX phosphorylation on Ser-139 in cells untreated by genotoxic agents is cell-cycle phase specific and attenuated by scavenging reactive oxygen species. *Int J Oncol*. 2006; 28:1491–505. [PubMed: 16685450]
44. McManus KJ, Hendzel MJ. ATM-dependent DNA-damage independent mitotic phosphorylation of H2AX in normally growing mammalian cells. *Molec Biol Cell*. 2005; 16:5013–25. [PubMed: 16030261]
45. Ichijima Y, Sakasai R, Okita N, Asahina K, Mizutani S, Teraoka H. Phosphorylation of histone H2AX at M phase in human cells without DNA damage response. *Biochem Biophys Res Commun*. 2005; 336:807–12. [PubMed: 16153602]
46. Oricchio E, Saladino C, Iacovelli S, Soddu S, Cundari E. ATM is activated by default in mitosis, localizes at centrosomes and monitors mitotic spindle integrity. *Cell Cycle*. 2006; 5:88–92. [PubMed: 16319535]
47. Hao LY, Strong MA, Greider CW. Phosphorylation of H2AX at short telomeres in T cells and fibroblasts. *J Biol Chem*. 2004; 279:45184–54.

48. Huang X, Kurose A, Tanaka T, Traganos F, Dai W, Darzynkiewicz Z. Sequential phosphorylation of Ser-10 on histone H3 and Ser-139 on histone H2AX and ATM activation during premature chromosome condensation: Relationship to cell-cycle and apoptosis. *Cytometry*. 2006; 69A:222–9. [PubMed: 16528736]
49. Juan G, Pan W, Darzynkiewicz Z. DNA segments sensitive to single strand specific nucleases are present in chromatin of mitotic cells. *Exp Cell Res*. 1996; 227:197–202. [PubMed: 8831556]
50. Darzynkiewicz Z, Traganos F, Sharpless T, Melamed MR. Different sensitivity of DNA in situ in interphase and metaphase chromatin to heat denaturation. *J Cell Biol*. 1977; 73:128–38. [PubMed: 16017]
51. Dobrucki J, Darzynkiewicz Z. Chromatin condensation and sensitivity of DNA in situ to denaturation during cell cycle and apoptosis. A confocal microscopy study. *Micron*. 2001; 32:645–52. [PubMed: 11334733]
52. Tanaka T, Kurose A, Huang X, Traganos F, Dai W, Darzynkiewicz Z. Extent of constitutive histone H2AX phosphorylation on Ser-139 varies in cells with different TP53 status. *Cell Proliferation*. 2006; 39:313–23. [PubMed: 16872365]
53. Achanta G, Huang P. Role of p53 in sensing oxidative DNA damage in response to reactive oxygen species-generating agents. *Cancer Res*. 2004; 64:6233–9. [PubMed: 15342409]
54. Zhou J, Ahn J, Wilson SH, Prives C. A role for p53 in base excision repair. *EMBO J*. 2001; 20:914–23. [PubMed: 11179235]
55. Offer H, Milyavsky M, Erez N, Matas D, Zurer I, Harris CC, Rotter V. Structural and functional involvement of p53 in BER in vitro and in vivo. *Oncogene*. 2001; 20:581–9. [PubMed: 11313990]
56. Al Rashid ST, Dellaire G, Cuddihy A, Jalali F, Vaid M, Coackley C, Folkard M, Xu M, Chen BPC, Chen DJ, Lilge L, Prise KM, Bazet Jones DP, Bristow RG. Evidence for the direct binding of phosphorylated p53 to sites of DNA breaks in vivo. *Cancer Res*. 2005; 65:10810–21. [PubMed: 16322227]
57. Tanaka T, Kurose A, Halicka HD, Traganos F, Darzynkiewicz Z. 2-Deoxy-D-glucose reduces the level of constitutive activation of ATM and phosphorylation of histone H2AX. *Cell Cycle*. 2006; 5:878–82. [PubMed: 16628006]
58. Roth GS, Lane MA, Ingram DK. Caloric restriction mimetics: The next phase. *Ann NY Acad Sci*. 2005; 1057:365–71. [PubMed: 16399906]
59. Lee J, Bruce-Keller AJ, Kruman Y, Chan SL, Mattson MP. 2-Deoxy-D-glucose protects hippocampal neurons against excitotoxic and oxidative injury: Evidence for the involvement of stress proteins. *J Neurosci Res*. 1999; 57:48–61. [PubMed: 10397635]
60. Halicka DH, Ardelt B, Li X, Melamed MR, Darzynkiewicz Z. 2-deoxyglucose enhances sensitivity of human histiocytic U 937 cells to apoptosis induced by Tumor Necrosis Factor. *Cancer Res*. 1995; 55:444–9. [PubMed: 7812976]
61. Parrinello S, Samper E, Krtolica A, Goldstein J, Melov S, Campisi J. Oxygen sensitivity severely limits the replicative lifespan of murine fibroblasts. *Nat Cell Biol*. 2003; 5:741–7. [PubMed: 12855956]
62. Schriener SE, Linford NJ, Martin GM, Treuting P, Ogburn CE, Emond M, Coskun PE, Ladiges W, Wolf N, Van Remmen H, Wallace DC, Rabinovitch PS. Extension of murine life span by overexpression of catalase targeted to mitochondria. *Science*. 2005; 308:1875–78. [PubMed: 15976292]
63. Darzynkiewicz Z, Traganos F, Melamed MR. New cell cycle compartments identified by multiparameter flow cytometry. *Cytometry*. 1980; 1:98–108. [PubMed: 6170495]
64. Darzynkiewicz Z, Sharpless T, Staiano-Coico L, Melamed MR. Subcompartments of the G<sub>1</sub> phase of cell cycle detected by flow cytometry. *Proc Natl Acad Sci USA*. 1980; 77:6696–700. [PubMed: 6161370]
65. Darzynkiewicz Z, Traganos F, Staiano-Coico L, Kapuscinski J, Melamed MR. Interactions of rhodamine 123 with living cells studied by flow cytometry. *Cancer Res*. 1982; 42:799–806. [PubMed: 7059978]



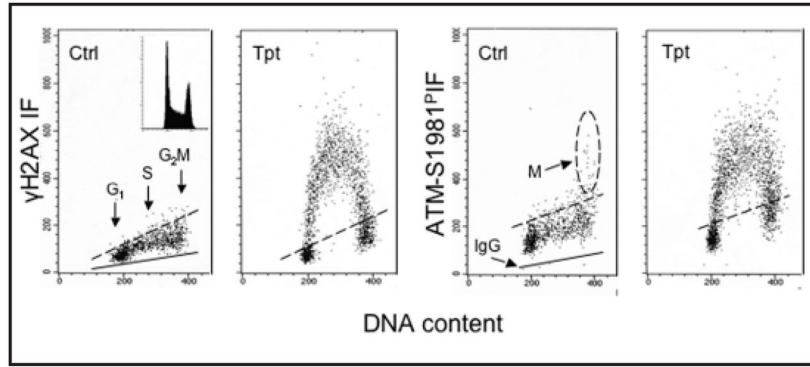


**Figure 1.**

Induction of H2AX phosphorylation and activation of ATM in HL-60 cells by the DNA topoisomerase I inhibitor topotecan (Tpt). Bivariate (cellular IF vs DNA content) distributions showing the selective response of S-phase cells to Tpt-induced DNA damage by histone H2AX *Ser139* phosphorylation and ATM activation (phosphorylation of *Ser1981*). Untreated (Ctrl) cells or cells exposed to 150 nM Tpt for 2 h were fixed and subjected to immunocytochemical detection of  $\gamma$ H2AX or ATM-S1981<sup>P</sup> concurrent with DNA content measurement by flow cytometry.<sup>41</sup> The inset shows the cellular DNA content frequency histogram from untreated culture; no significant changes in the cell cycle distribution was apparent during exposure to Tpt. The solid lines represent the upper level of the fluorescence intensity of the control cells stained with an irrelevant isotype IgG instead of the specific primary Ab. Dashed lines show the upper limit of IF (maximum level for >95% of interphase cells) of the untreated cells. However, mitotic (M) cells from untreated cultures show the presence of activated ATM.<sup>43-47</sup> Note selective response of S-phase cells to the drug.

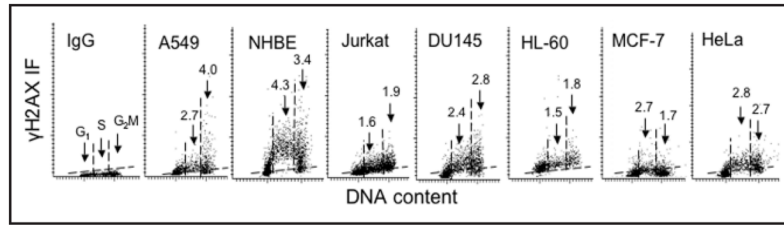


**Figure 2.**

Different levels of CHP in different cell types in relation to cell cycle phase. Bivariate distributions (scatterplots) of cellular DNA content vs  $\gamma$ H2AX IF of human cells from exponentially growing untreated lung adenocarcinoma A549, normal bronchial epithelial (NHBE), T-cell leukemic Jurkat, prostate carcinoma DU145, leukemic HL-60, breast carcinoma MCF-7 and cervical carcinoma HeLa cell cultures measured by laser-scanning cytometry, as described.<sup>43</sup> The negative isotype control (IgG; A549 cells) is shown in the panel on the left; the maximal level of IgG IF, below which >97% cells in the IgG panel were located, is marked in each panel with a broken line (other cell types had similarly low IgG IF). The vertical dashed lines show the gates used to separate G<sub>1</sub>, S and G<sub>2</sub>M cell subpopulations to obtain their mean values of  $\gamma$ H2AX IF. The figures above the arrows pointing to S and G<sub>2</sub>M cells indicate the n-fold higher mean expression of  $\gamma$ H2AX of S and G<sub>2</sub>M phase cells, respectively, compared to G<sub>1</sub> cells, whose mean  $\gamma$ H2AX (for each cell type) was normalized, to 1.0.

\$watermark-text

\$watermark-text

\$watermark-text

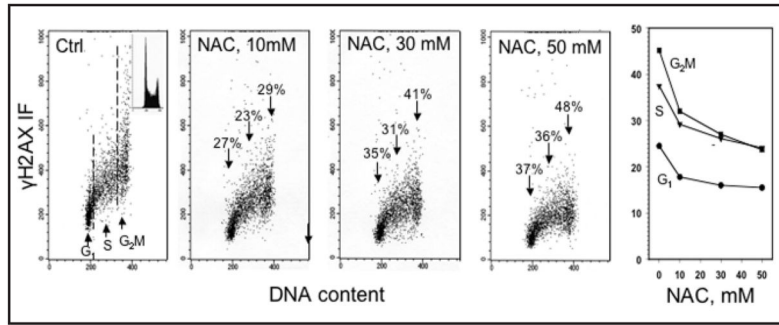


**Figure 3.**

Decrease in CHP in TK6 cells induced by their treatment with different concentration of NAC. The bivariate (DNA content vs  $\gamma$ H2AX IF) distributions illustrate CHP of cells growing in the absence (Ctrl) or presence of 10, 30 or 50 mM NAC, added into cultures for 1 h prior to cell harvesting. The DNA content frequency histogram representative of the cell in these cultures is shown in the inset of the left panel. The percent decrease in mean values of  $\gamma$ H2AX IF of G<sub>1</sub>, S and G<sub>2</sub>M phase cell populations in cultures treated with NAC in relation to the untreated (Ctrl) cells are marked above the arrows pointing out towards the cells in the respective phases of the cycle. The plot of the mean values of  $\gamma$ H2AX IF for G<sub>1</sub>, S and G<sub>2</sub>M cell populations, estimated by gating analysis, as a function of NAC concentration, is shown in the right panel. For details see reference 41.

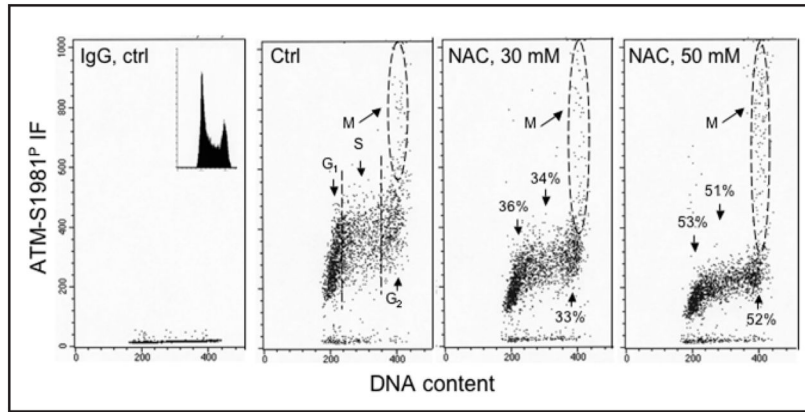


**Figure 4.** Decrease in CAA in TK6 cells treated with different concentrations of NAC. The bivariate (DNA content vs ATM-S1981<sup>P</sup> IF) distributions illustrate CAA of cells growing in the absence (Ctrl) or presence of 30 or 50 mM NAC included into cultures for 1 h prior to cell harvesting. The left panel shows the IgG isotype (negative) control; the DNA content frequency histogram representative of the cell in these cultures is shown in the inset of this panel. Mitotic cells (M) have a high level of ATM-S1981<sup>P</sup> IF<sup>43–47</sup> and are marked by the oval dashed-line boundaries. The percent decrease in mean values of CAA of G<sub>1</sub>, S and G<sub>2</sub> (M cells excluded) cell populations in cultures treated with NAC in relation to the untreated (Ctrl) cells are marked above the arrows pointing out towards the cells in the respective phases of the cycle.

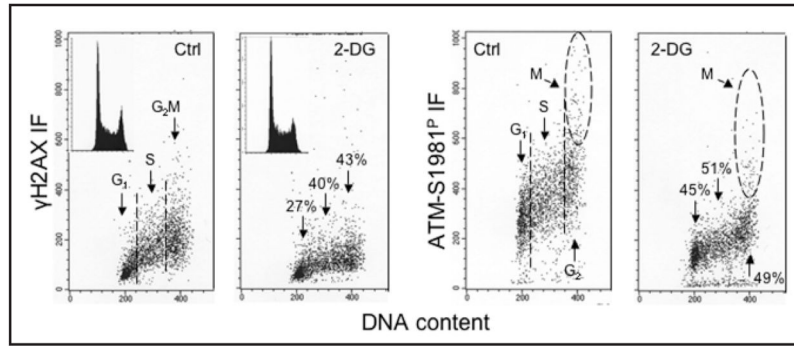


**Figure 5.**

Decrease in the level of CHP and CAA in human lymphoblastoid NH32 cells grown in the presence of 2-deoxy-D-glucose (2-DG). The bivariate (DNA content vs  $\gamma$ H2AX, or vs ATM-S1981<sup>P</sup>) distributions of untreated cells (Ctrl), and cells growing in the presence of 5 mM 2-DG for 24 h. The DNA content frequency histograms, representative of the untreated and treated cells, are shown in the respective insets. Mitotic cells (M) express high level ATM-S1981<sup>P</sup> IF which appears unrelated to endogenous DNA damage-induced CAA.<sup>42–45</sup> The percent decrease in mean values of  $\gamma$ H2AX IF or ATM-S1981<sup>P</sup> IF of G<sub>1</sub>, S, and G<sub>2</sub>M phase cell populations (only G<sub>2</sub> phase cells in the case of ATM-S1981<sup>P</sup>) in cultures treated with 2-DG in relation to untreated (Ctrl) cells is listed above or below each arrow pointing towards the cells in the respective phases of the cycle.

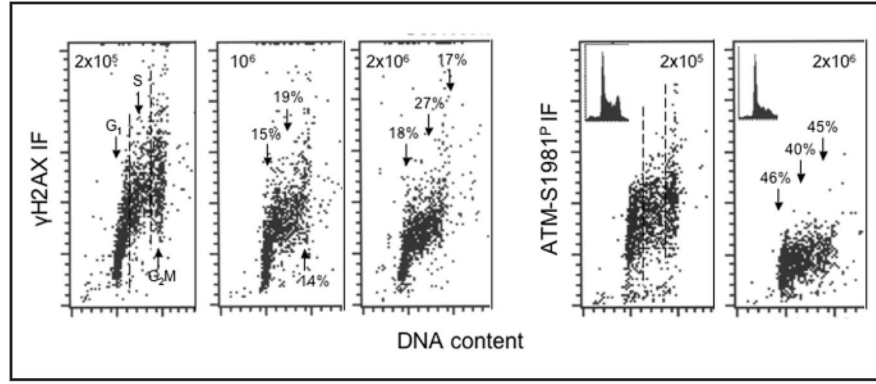


**Figure 6.**

Decreased levels of CHP and CAA in TK6 cells growing at higher cell densities. Human lymphoblastoid TK6 cells were seeded in cultures at different densities and were harvested when the densities approached  $2 \times 10^5$ ,  $10^6$  or  $2 \times 10^6$  cells/ml. The bivariate (DNA content vs  $\gamma$ H2AX, or vs ATM-S1981<sup>P</sup>) distributions illustrate a decline in CHP and CAA of cells growing at higher densities. Insets in the right panels show DNA content histograms in these cultures. The percent decrease in mean values of  $\gamma$ H2AX IF or ATM-S1981<sup>P</sup> IF of G<sub>1</sub>, S and G<sub>2</sub>M cell populations in cultures at  $10^6$  or  $2 \times 10^6$  cells/ml with respect to the cells growing at density  $2 \times 10^5$  cells/ml is shown above each arrow pointing towards the cells in the respective phase of the cycle.